Supplementary Information

Novel magnetic HS⁻-adsorptive nanocomposite photocatalyst (rGO/CoMn₂O₄-MgFe₂O₄) for hydrogen fuel production using H₂S feed

Majid Ghanimati [a], *Mohsen Lashgari* [* a,b], *Fabio Montagnaro* [c]*, Vassilios Binas* [d]*, Michalis Konsolakis* [e]*, Marco Balsamo* [c]

[a] Department of Chemistry, Institute for Advanced Studies in Basic Sciences (IASBS), Zanjan 45137-66731, Iran

[b] Center for Research in Climate Change and Global Warming: Hydrogen and solar division, Zanjan 45137-66731, Iran

[c] Department of Chemical Sciences, University of Naples Federico II, Complesso Universitario di Monte Sant'Angelo, 80126 Napoli, Italy

[d] Institute of Electronic Structure and Laser (IESL), FORTH, Vasilika Vouton, GR-70013Heraklion, Greece

[e] School of Production Engineering and Management, Technical University of Crete, GR-73100, Chania, Greece

* Corresponding author. Tel.: +98 24 33153205; fax: +98 24 33153232. *E-mail address:*
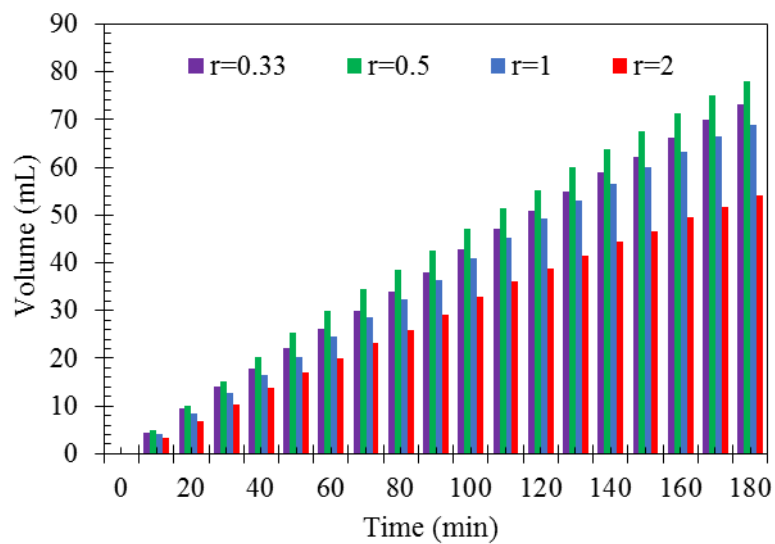
Lashgari@iasbs.ac.ir

Figure S1. The ability of the $x\text{CoMn}_2\text{O}_4$-$y\text{MgFe}_2\text{O}_4$ composite photocatalysts synthesized in this work ($r = \frac{x}{y}$: 0.33, 0.5, 1, and 2) to produce hydrogen gas [T=298 K, reaction medium: 50 mL alkaline H_2S feed (pH=11), photocatalyst mass: 0.2 g, light intensity: 1 sun].
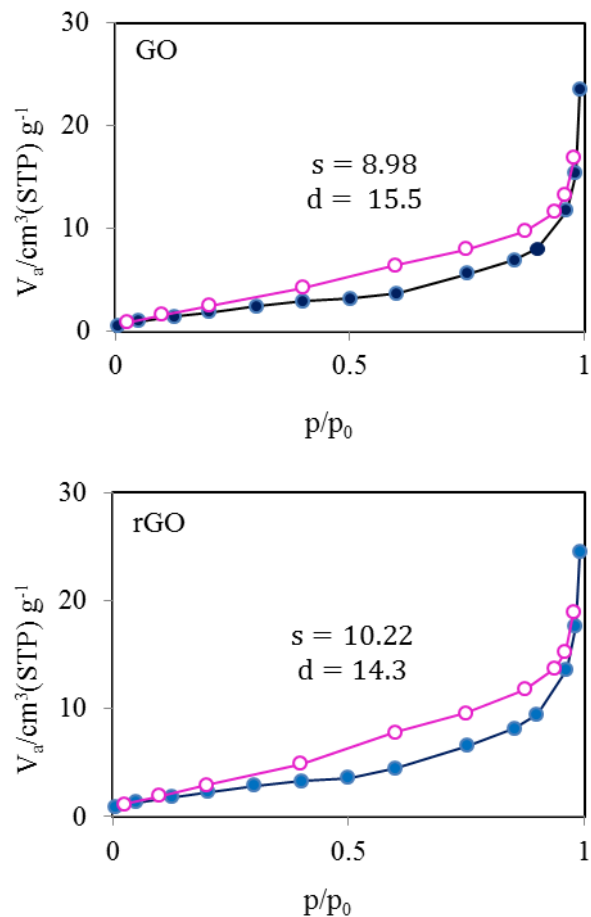
**Figure S2.** Nitrogen adsorption-desorption isotherms of GO and rGO (s: surface area (m^2 g^{-1}), d: mean pore diameter (nm). Solid and hollow circles are standing for adsorption and desorption processes, respectively).

The above diagrams show a hysteresis loop for both GO and rGO compounds. The observation of such a loop is a characteristic of mesoporous compounds (pore diameter: between 2 and 50 nm). The increase in surface area due to the conversion of GO to rGO, has also been witnessed elsewhere [see refs 59 and 60 of the main text].
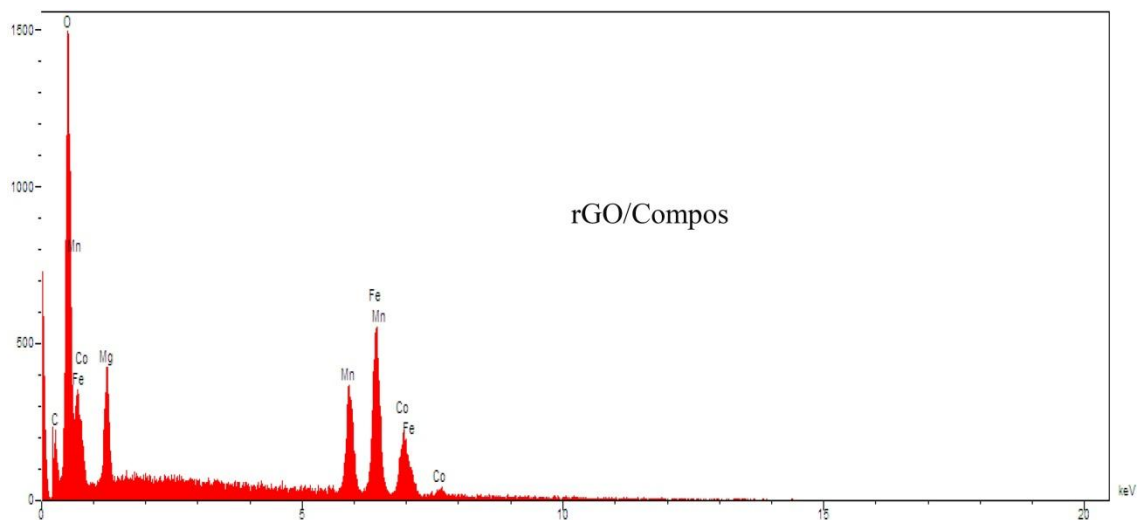
CoMn$_2$O$_4$

MgFe$_2$O$_4$

Compos

3
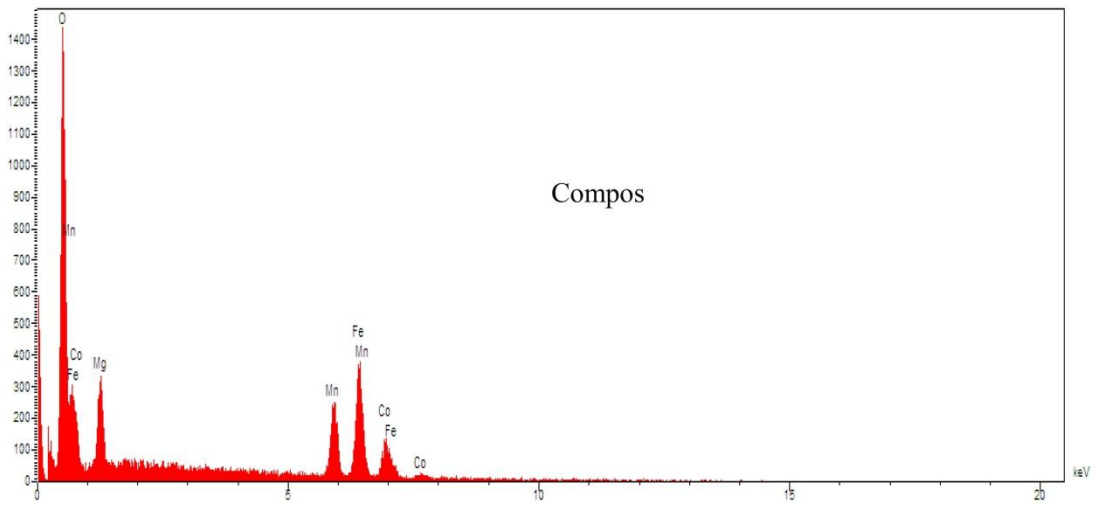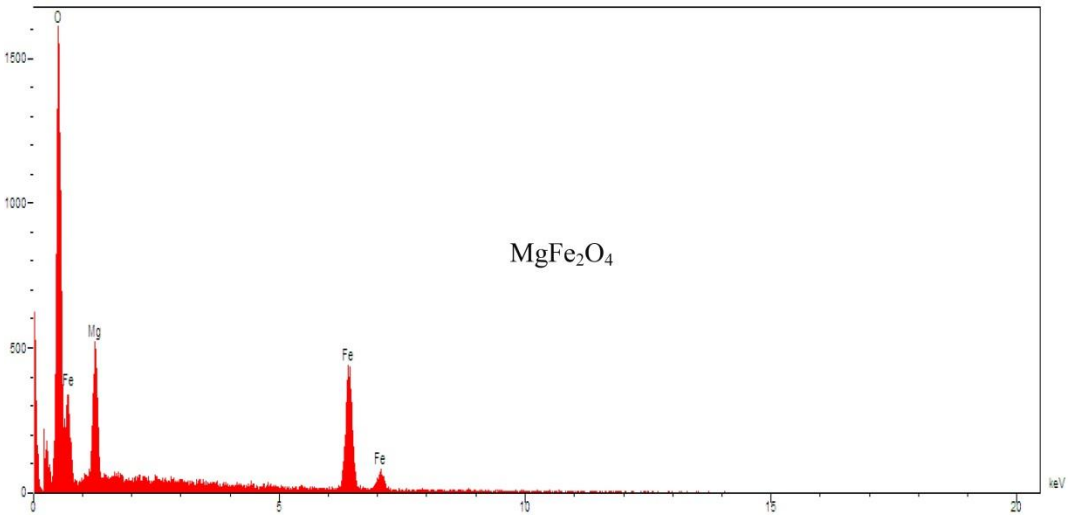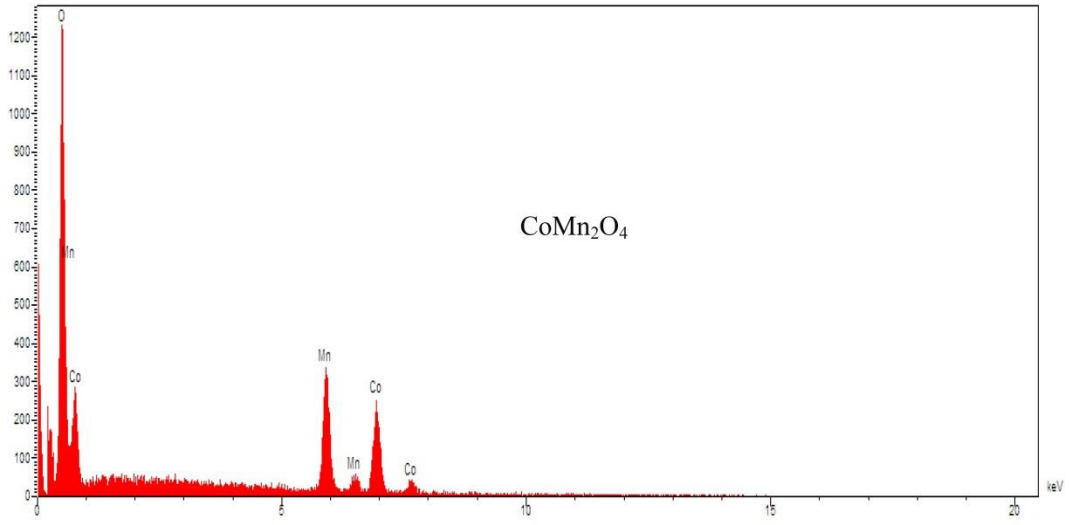
Figure S3. Energy dispersive X-ray (EDX) spectra of the $CoMn_2O_4$ and $MgFe_2O_4$ as well as their composite in the absence and presence of reduced graphene oxide (rGO).
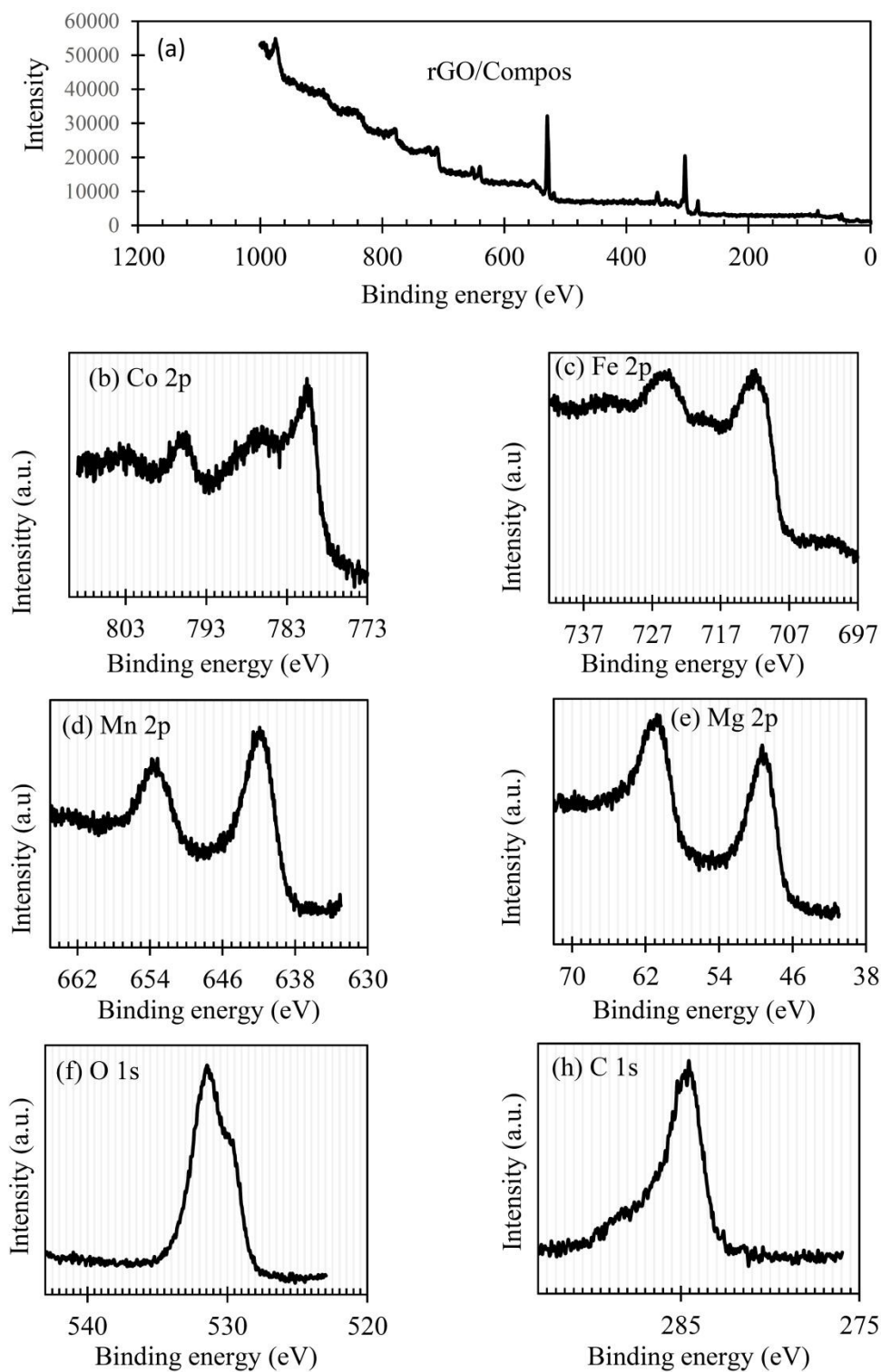
Figure S4. XPS spectra of the composite rGO/Compos photocatalyst: (a) survey, (b) Co, (c) Fe, (d) Mn, (e) Mg, (f) O, and (g) C spectra.
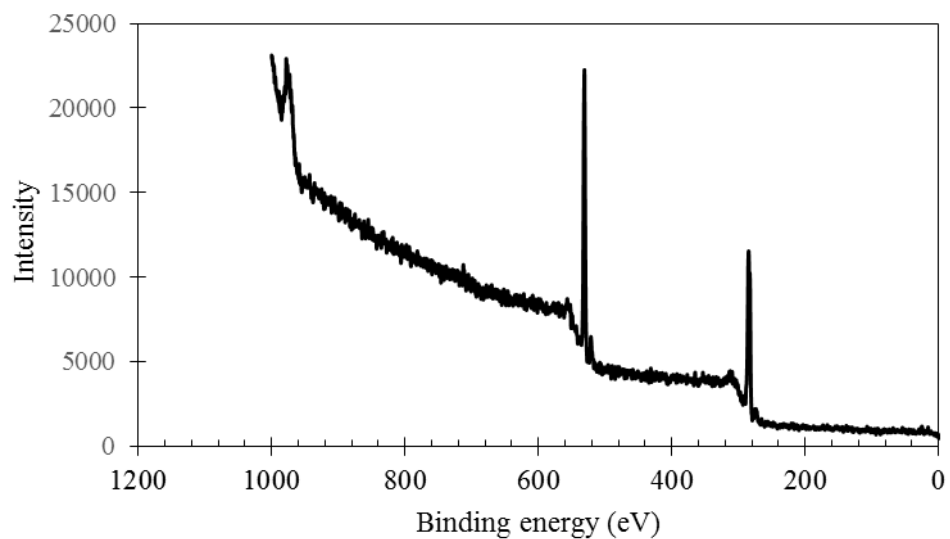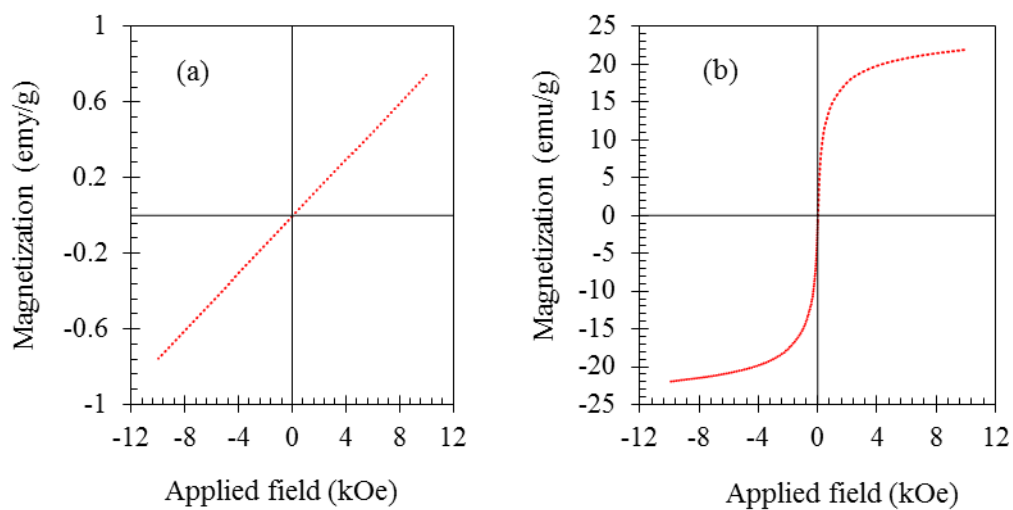
Figure S5. XPS survey of rGO.

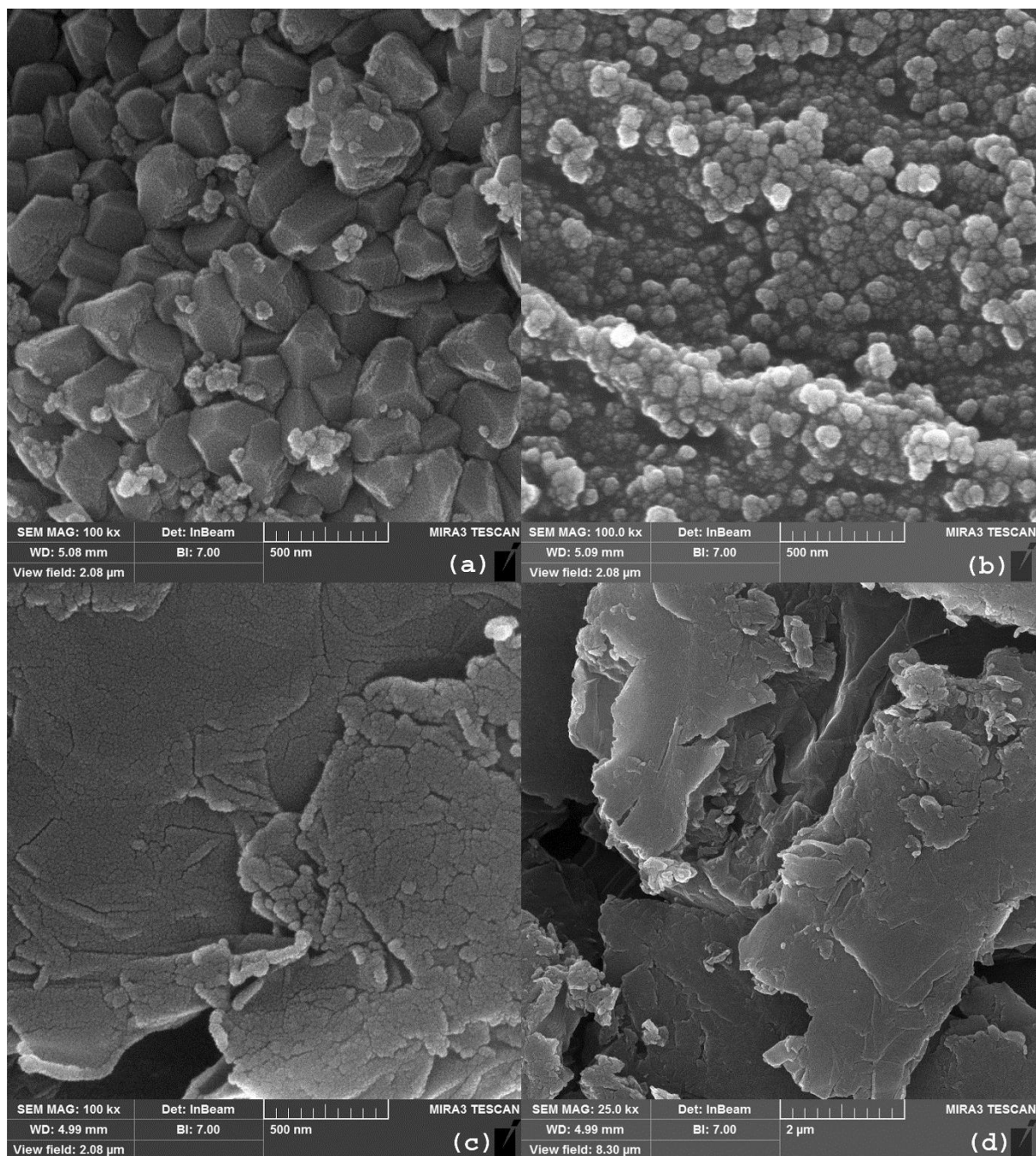**Figure S6.** Magnetic hysteresis loop recorded for the Compos components, i.e. $CoMn_2O_4$ (a) and $MgFe_2O_4$ (b).

Figure S7. FESEM images of CoMn$_2$O$_4$ (a), MgFe$_2$O$_4$ (b), and GO (c, d).

This figure shows that the CoMn$_2$O$_4$ synthesized in this work is composed of a series of polyhedral nanoparticles (**Fig. S7a**), and MgFe$_2$O$_4$ consists of almost uniform nanoparticles (**Fig. S7b**). The graphene oxide (GO) has also a layered nano-flake/plate structure, stacked together (**Figs S7c** and **S7d**). The SEM images observed for these compounds are consistent with the structures reported in the literature [ref. 61 of the main text; C. Lin et al, *Nanomaterials* 9 (2019) 774; M. Kooti et al, *Appl. Microbiol. Biotechnol.* 102 (2018) 3607].
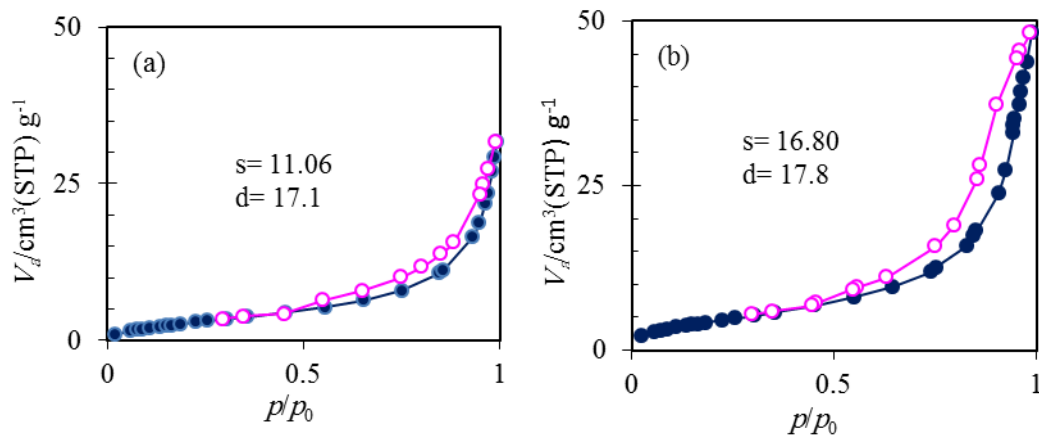
Figure S8. Nitrogen adsorption-desorption (BET) isotherms of $CoMn_2O_4$ (a) and $MgFe_2O_4$ (b) photocatalyst components (s: surface area (m^2 g^{-1}), d: mean pore diameter (nm). In these diagrams, solid and hollow circles denote the N_2 adsorption and desorption processes, respectively).
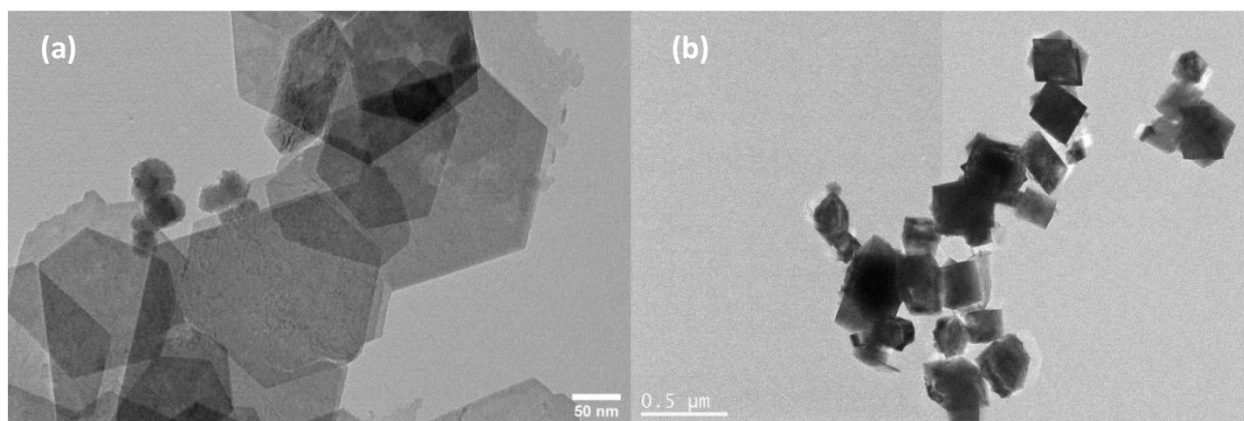
Figure S9. HRTEM images of the Compos components: a) $CoMn_2O_4$ and b) $MgFe_2O_4$.
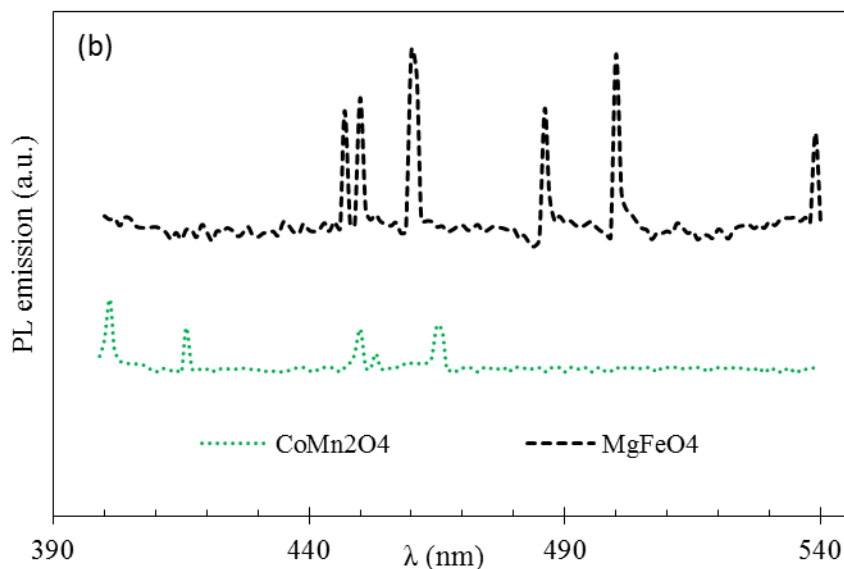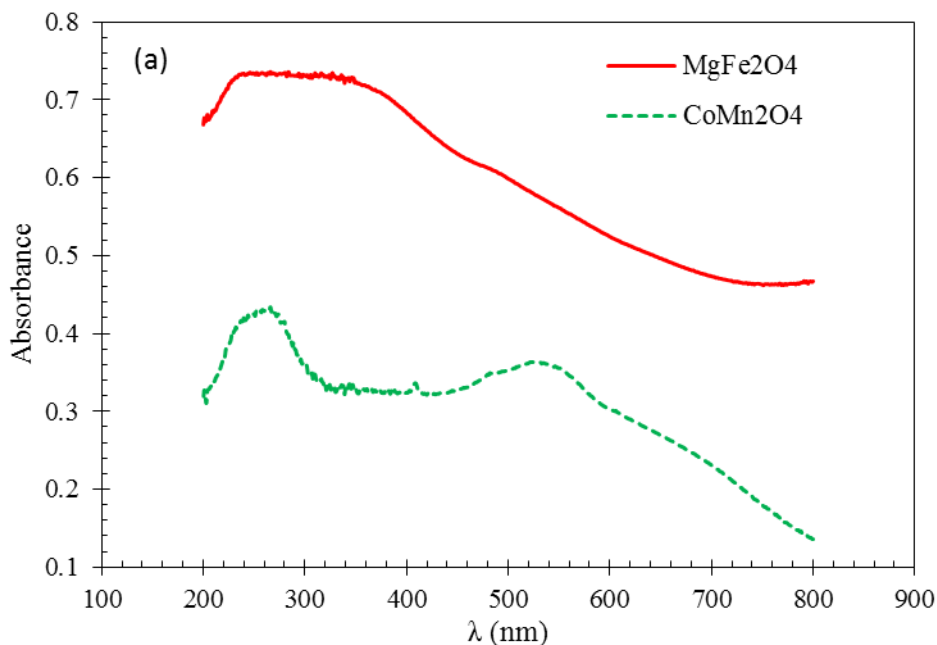
Figure S10. Diffuse reflectance (DR) UV-visible (a) and photoluminescence (PL; b) spectra of the photocatalyst components, i.e. $CoMn_2O_4$ and $MgFe_2O_4$.

Figure S10a exhibits superior light absorbance for $MgFe_2O_4$. By contrast, a lower PL emission is observed for $CoMn_2O_4$ (**Fig. S10b**), indicating less charge recombination for this compound compared to $MgFe_2O_4$. It should also be noted that the PL emission peaks observed for $MgFe_2O_4$ (around 447, 450, 460, 486, 500, and 539 nm) and $CoMn_2O_4$ (around 400, 416, 450, 453, 465 nm) are characteristic emissions of these compounds, reported in the literature [ref. 23 of the main text; N. Kaur et al, *Ceram. Int.* 44 (2018) 4158-4168; K. Shetty et al, *Physica B* 507 (2017) 67-75; G. Vaish et al, *J. Mater. Sci.: Mater. Electron.* 30 (2019) 16518-16526].
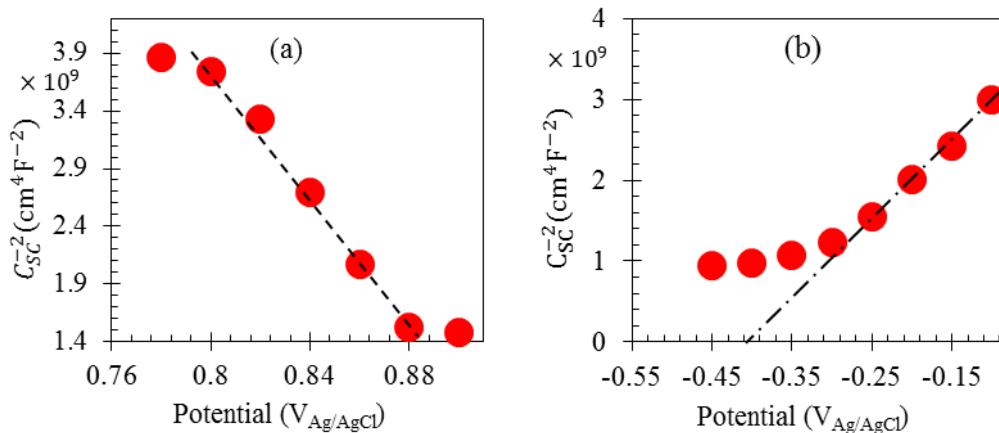
Figure S11. Mott–Schottky (MS) diagrams of the $CoMn_2O_4$ (a) and $MgFe_2O_4$ (b) semiconducting materials.

The negative and positive MS slopes observed for $CoMn_2O_4$ and $MgFe_2O_4$ clearly indicate that these materials are p- and n-type semiconductors, respectively (see refs 73 and 87 of the main text).
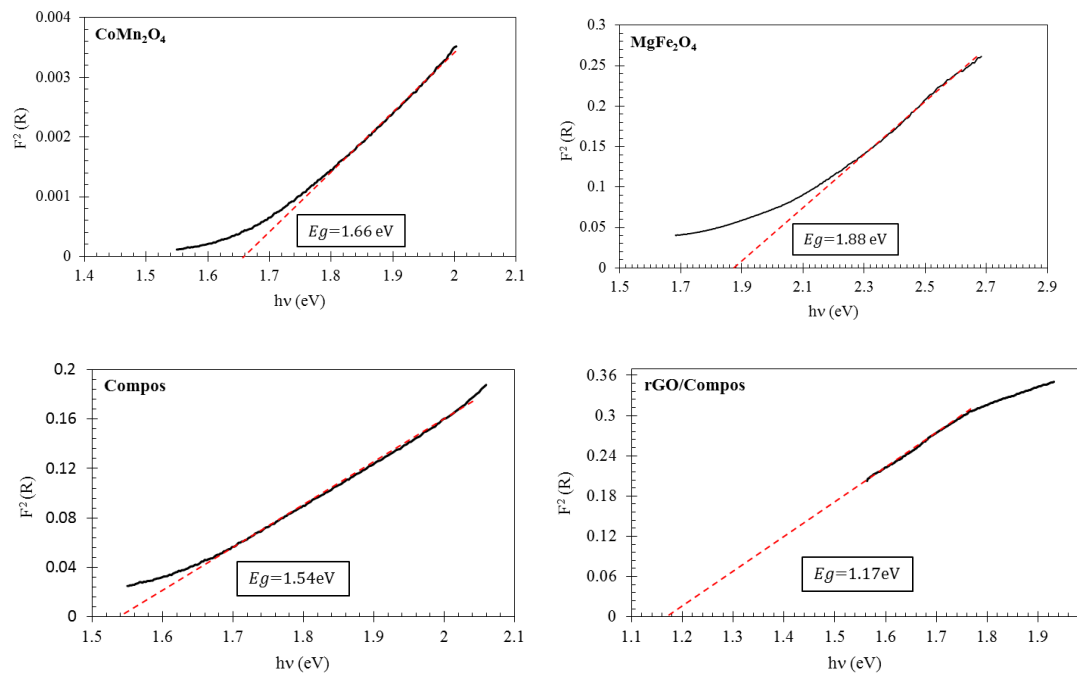
Figure S12. Kubelka-Munk diagrams for bandgap determination of the photocatalyst materials under consideration.

Table S1: The extent of sulfur adsorbed by the Compos components in the alkaline sulfide solution (0.5 M, initial pH: 11).

Component	S (wt. %)	pH*
$CoMn_2O_4$	12.86	12.00
$MgFe_2O_4$	0.22	11.22

* measured at the end of the adsorption process.